An Improved Control Technique for Grid Interactive 4-Phase SRM Driven Solar Powered WPS Using Three Level Boost Converter

[1]N. S. V. Sai kumar*, PG student, St. Marys group of institutions, Guntur, AP, India*
[2]Lakshmi Narayana*, HOD, St. Marys group of institutions, Guntur, AP, India*

Abstract: *In this project a three level boost converter with 8/6 SRM drive is presented for solar based water pumping system. The Solar power boost converter system is integrated with the single phase grid system in order to utilize the excessive energy generated by the solar system. The main aim of the grid integration is to save excess power to earn money for the consumer. Additionally, it also balances the power supply fluctuations if any, to drive the motor smoothly. A new control strategy is developed to regulate the DC link voltage properly and to control the grid inverter system effectively. As compared with conventional boost converter, A three level boost converter is adopted for the proposed system for neutralizing split capacitor voltage unbalances. Besides, this converter is operated with MPPT controller to maximize the solar power. The proposed system is designed in MATLAB SIMULINK software to test its performance.*
Keywords: *Solar powered system, 8/6 SRM, Grid integration, Three level boost converter*

I. INTRODUCTION

A continuous price declination of solar photovoltaic (PV) panels and power electronics components, has stimulated the researchers and industries to utilize the solar power for various applications [1]. Water pumping in many sectors, which may comprise but not restricted to, agriculture purposes, drinking water supply, fountaining and water supply to the industries, has gained a wide consideration as a decisive and inexpensive application of the solar PV array power [2-3]. Although the standalone solar powered systems have various advantages, the intermittency in supply and inadequacy to deliver full valued requisite power to the drive at night or in cloudy days incapacitate its merits [4].

One of the ways to overcome this constraint is by associating the battery with the water pumping system [5]. Nevertheless, the association of a battery energy storage (BES), decreases the service life, makes the system costly and increases the maintenance necessities. Hence, it is valuable to utilize the pump-storage, which stores PV energy as the potential energy in a water reservoir to be utilized according to the demand [6]. Another efficient solution to overcome this incompetency of standalone SPWPS can simply be resolved by integrating a grid to the system [7]. A grid synchronized SPWPS ensures no power intermittent even under low solar irradiation, cloudy days or in evening time [8]. The additional power required by the pump, when the solar PV array is inept of providing the required power, it is supplied by the utility grid. Further, the utility grid integrated into the system improves the reliability and efficacy of the pumping system. However, no such arrangement with an SRM is reported until now.

The SRM drive has gained widespread attention over other conventional and permanent magnet (PM) motors, since the last few years for a solar-powered water pumping system [9-10]. The attractive features of this drive, comprise a high efficiency, compact structure, easy to construct, inexpensive, high torque/inertia ratio and wide speed range operation capability [11]. Some of the literature have also discussed the use of synchronous reluctance motor (SyRM) in a solar-powered water pumping system. The rotor construction of SyRM is simple in comparison to either the induction motors (IMs) or permanent magnet (PM) motors due to the absence of magnets and a cage. However, it is costlier than the IM and needs speed synchronization to the inverter output frequency and requires the complex control to drive the motor. The SyRM has also a poor power factor, and therefore, the kVA rating of the inverter is large. Therefore, SRM drive is implemented in this work, which has additional advantageous over other available drives. The rotor size of SyRM is also nearly 15% more than SRM. The other benefits of SRM, include the capability to operate over a wide temperature range without performance degradation due to the absence of magnets, unipolar phase energization, it needs a minimum of one switch/phase, the converter is immune to shoot-through faults, etc. [12-13]. In order to utilize these benefits, many researchers have examined and analyzed the performance of SRM drive in standalone solar-based water pumping system [14-17]. But all of them, have suffered from the common problem of solar power intermittency

---

and underutilization of the system. However, one such arrangement in which the standalone 4-phase SRM driven water pumping system integrated with the grid is given in [18]. Although, the system is able to offer the continuous water supply against its full capacity, the asymmetric split capacitors converter has a serious constraint of voltage inequity across its two split capacitors. This asymmetry causes a need for large DC link capacitors for stabilizing the desired DC-link voltage and also generates a high ripple in the current and torque of the drive. In addition, the drive also fails to start in some cases due to the presence of high asymmetry in voltages.

Therefore, recognizing the limitations of conventional systems, this work proposes an optimal configuration with an efficient power management scheme of grid-interactive SPWPS utilizing a 4-phase SRM drive with a mid-point converter as shown in Fig.1. This multifunctional configuration aims at the design of a reliable and cost-effective water pumping system with a grid synchronized PV array unit employing 4-phase SRM motor-pump for the first time. When the PV array is incompetent to provide the required power to drive for the full discharge of water, the utility grid acts as a backup source and provides the remaining power to the system. Using a single-phase voltage source converter (VSC), a control logic alterations incorporating the combined second and third-order generalized integrator (HSTOGI) controller [19] accomplishes a bidirectional power flow control between the grid and the DC link of a mid-point converter, which feeds the power to SRM. Various filters are reported in the literature to extract the fundamental voltage from the grid supply. Due to the involvement of numerous fundamental voltage computations, the conventional techniques have a time lagging response [20-22]. The second-order generalized integrator (SOGI) filter has a fast response and ability to mitigate the phase and frequency inaccuracy while extracting fundamental terms. However, there is a problem with DC offset in this filter [21]. A notch filter based third-order filter (TOGI) is discussed in [22]. Although, the response of this filter is better than SOGI, it has small attenuation for DC offset voltage present in the supply side. Thus, the developed control for grid-side VSC has incorporated a hybrid of both the previously mentioned filters and, therefore, has the benefits of both the filter with enhanced eliminating capability for high and low-frequency harmonics. In addition, the PV array side control logic is also implemented to achieve two key aspects, first is performance optimization of the solar PV and another is to offer a similar voltage to the DC link capacitors of a mid-point converter. The motor side control is also associated with a soft-stating control logic such that a limited starting inrush current is flowing through the motor windings at starting condition when back EMF is zero.
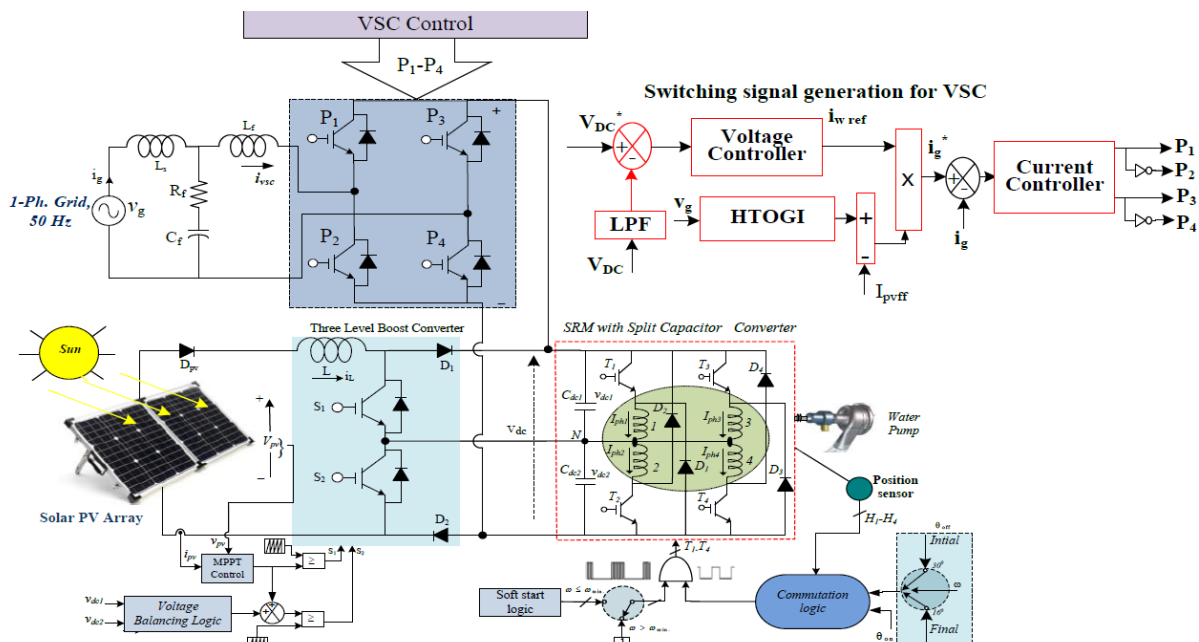
II.   PROPOSED SYSTEM

Fig. 1 Circuit diagram of grid interfaced solar-powered water pumping system

2.1 System configuration

A developed solar-powered water pumping system with grid support utilizing a 4-phase switched reluctance motor is presented in Fig. 1. The PV array with sufficient power (at STC) is used to run the water pump at its full capacity irrespective of the presence or absence of grid supply. The three-level boost converter (TLBC) performs the MPPT operation and voltage balancing across split capacitors, whereas the mid-point

converter performs an electronic commutation of SRM drive at the fundamental frequency. The inbuilt four Hall-Effect sensors are mounted on the stator and are utilized to generate the position signals to successfully operate the electronic commutation of SRM drive. A single-phase grid is connected to the DC link through voltage source converter (VSC). The control of VSC enables a bi-directional power transfer at DC link capacitors.

2.2 Design of developed system
Different working stages and components such as solar PV array, dual output boost converter, a mid-point converter, SRM-pump, single-phase utility grid, common DC link capacitor, R-C filter, and an interfacing inductor, are used in the proposed system. A 750 W, 1500 rpm @ 310 V SRM is selected in the system. A single-phase grid at a 50 Hz utility grid is connected at the DC link to provide the back-up to the system. Depending on these selections, other components and parameters are estimated, as described in the following sections.

2.3 Design of Solar Panel
An HBL-Solar Company makes PV module with a maximum power point (MPP) voltage and current of 18.65 V and of 4.01 A, respectively, is selected to realize a solar panel of requisite power. The higher value of duty ratio, '*D*' causes an increase in the inductor current rating and a poor switch utilization. An optimized value of duty ratio, 0.29 is selected to develop the solar panel side MPPT converter. As the output voltage of a boost converter is consistently regulated at a predefined value, regardless of the operating conditions. The variation in the duty ratio of the boost converter is considerably less under any variation in the atmospheric condition. Thus, the solar panel is selected such that the single input dual output boost converter is worked at a comparatively much lower value of duty ratio even under STC. The complete specifications of solar panel indices and the number of series and parallel connected modules are given in the Appendix.

2.4 Design of Three-Level Boost Converter (TLBC)
The TLBC is an important component of the developed system and it is very important to design its parameters carefully. Its design is mainly governed by the sizing of input inductor, '*L*'. The value of an inductor, L is chosen such that the TLBC is permanently working in a continuous inductor current mode (CICM) so that there is reduced stress on converter indices. The design of TLBC is done at rated condition i.e. at 1000W/m2 and therefore, the duty ratio, D required to estimate the size of inductor is computed as [23],
There is a valid reason behind opting for the particular design of the PV array for a given configuration. Generally, in a conventional standalone solar powered SRM driven water pumping system, the DC link voltage is kept variable and the drive speed is regulated by available solar power. As solar power decreases, there is a decrement in the duty ratio. There is always be a possibility that the value of the duty cycle can hit the zero value at lower insolation levels and the solar panel operation goes into non-MPPT mode. To avoid this situation, the rating of solar panel indices is selected such that the boost converter works in a range of value 0.5 to 0.6 at standard condition, away from zero, in order to retain the MPPT operation even at lower insolation levels. However, such a selection of duty ratio (moving far away from zero) causes an increase in the inductor current rating and a poor switch utilization. The aforesaid issues with standalone topology, using a three-level boost converter, do not exist with the proposed system. In this proposed topology, the PV array is designed, for a good switch utilization and a reduced inductor current rating of the TLBC. As the output voltage of a boost converter is consistently regulated at a predefined value, irrespective of the working situations, variation in the duty ratio of the TLBC is considerably less under any variation in the environmental condition. Thus, the solar panel is designed such that the converter functions at a comparatively much lower value of duty ratio even under STC. The MPPT is consistently achieved, as the duty ratio does not reach zero in any case. Therefore, the size of inductor for CCM operation is computed as [23], Where, '*fsw*' is the switching frequency of TLBC switches; 'ΔiL' is an amount of permitted current ripple through '*L*'.

2.5 Design of Grid Side VSC
The control developed for grid-tied VSC is utilized to facilitate the seamless power flow within the system. The maximum switch stress (blocking voltage) across grid-tied VSC integrated with the utility grid, is approximately equal to the DC link voltage, i.e. 310V. The voltage rating of the IGBT devices of VSC while considering the safety factor of 1.4.

III. CONTROL OF PROPOSED SWP SYSTEM
The proposed configuration has some control logic to work it properly and efficiently under all possible working conditions. These control techniques govern the operation of various stages like solar panel unit with MPPT converter and voltage balancing, a mid-point converter energized SRM-pump system and grid side VSC

control for the bidirectional power flow. A detailed discussion about these control techniques, is given in the coming sections.

3.1 PV Array Power Maximization and Voltage Balancing

Since, the SRM drive with a mid-point converter, has many benefits in comparison to other combinations. However, this arrangement has one elementary problem of voltage unbalancing across split DC link capacitors of a mid-point converter. Therefore, the dedicated control logic is required in such an SRM drive to take care of asymmetry compensation of voltages across these capacitors. In order to overcome this problem along with MPPT operation, the simple and reliable control logic is developed to look over both the operations under all possible working situations. The logic developed to achieve these desired operations is shown in Fig. 2. In this logic, the voltage across both the split DC link capacitors, ('*vdc1*', '*vdc2*') are compared throughout the operation and it makes the difference zero through voltage controller. The output of this controller is in the form of incremental duty ratio, 'Δd', which is amalgamated with the duty cycle produced by the PV array power optimization controller, '*D1*' i.e. '*D1 + ' '*. Finally, the resultant duty cycle is compared with a high-frequency triangular signal to generate the switching pulses for the lower switch, '*S2*' of the TLBC. Besides, the switching pulses for the upper switch, '*S1*' is simply generated by comparing '*D1*'with train of high frequency switching pulses.
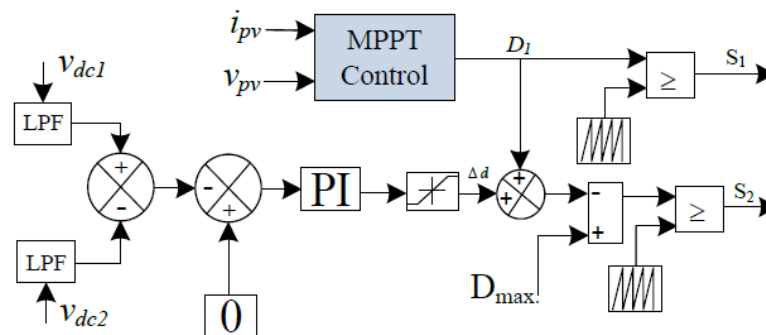

Fig. 2 Developed control logic for TLBC

3.2 Soft-Starting Technique and Speed Regulation

Since, the developed water pumping system avoids the current sensors at the motor side, the soft-starting of the drive is provided by controlling the starting current through PWM switching of an SRM converter for a certain speed. The logic to access the controlled starting current is represented in Fig. 3. As the magnitude of back-EMF is zero at standstill condition. Therefore, it is obligatory to start the motor with a controlled starting current. Since this SRM drive avoids winding current sensing, the starting current is controlled by regulating the rise of DC-link voltage through modulating the pulse duration of switching devices for a predefined duration. This switching time is assessed established on the inertia of the motor-pump system. The pulse width of an original pulse is modulated by a manually generated pulse train with a slowly increasing pulse width.

This leads to a controlled rate of rising of winding current. Once an appropriate back-EMF is produced, the motor is automatically switched into fundamental frequency mode or PWM mode depending upon the availability of solar power.
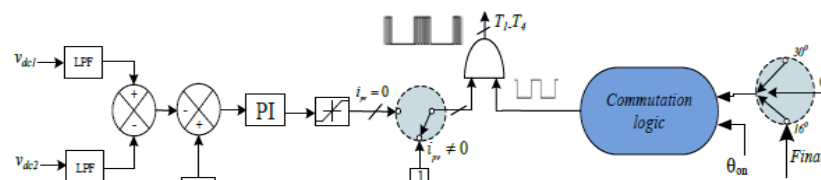

Fig.3 Soft-start logic of proposed SRM drive.

3.3 Grid Side VSC Control

A combination of the HSTOGI filter dependent control technique is used to switch the grid side VSC and to extract the fundamental voltage signal under any disturbances. The HSTOGI filter incorporated in the control scheme for grid-side VSC, needs the tuning of a single damping parameter, '*Ks*' and has the characteristics of the band-pass filter (BPF).

3.3.1 *Amplitude and Template Assessment of Supply Voltage*

The in-phase component of the voltage template with supply voltage is the coordinating signal, while, the quadrature component is used to estimate the peak value of grid voltage. The peak magnitude of grid voltage is then computed using these two signals as, where, '*vsp*' is the in-phase and '*vsq*' is the quadrature component of the grid voltage. The PV array power feeds to the grid is at unity power factor and active in nature. The expression to estimate the in-phase component is as,
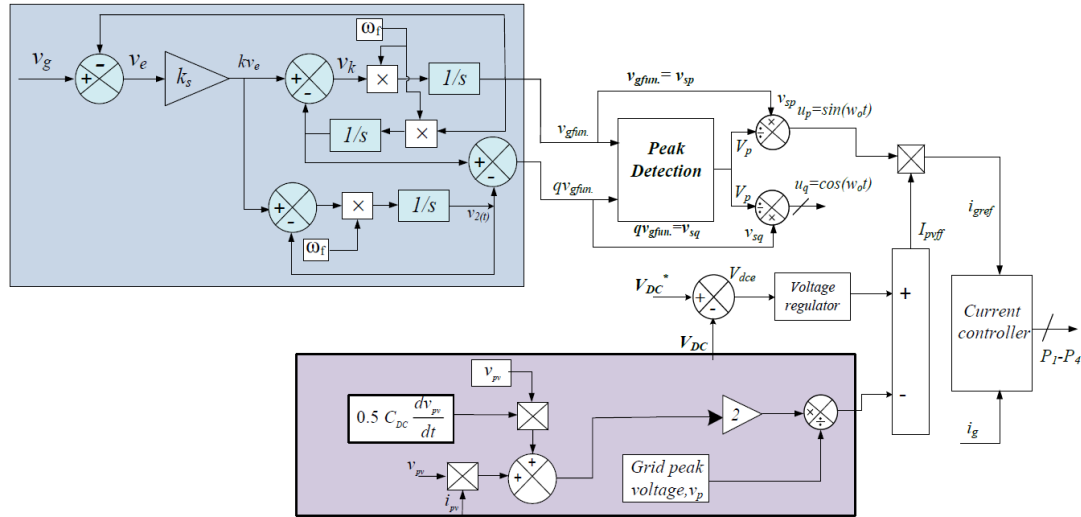

Fig 4 Control scheme for grid-side VSC

3.3.2 *Assessment of Active Loss Component*

The amount of power drawn from the grid to the drive is governed by the difference in actual and desired DC link voltages. The grid side VSC has also a function to control the desired DC-link voltage such that the SRM drive is always working at fundamental switching frequency irrespective of the working condition.

As shown in Fig. 4, the reference value of DC-link voltage '*vdc**' is compared with the sensed voltage '*vdc*' after passing through the low pass filter (LPF) to generate an error voltage '*vdce*' as,

This difference in two voltages, is given to the proportional-integral (PI) controller to compute the active loss term, '*Iloss*'. The PI controller output, '*Iloss*', which is basically a voltage regulator, is computed as,

3.3.3 *PV Deflection Term*

For improving the dynamic performance of the system under solar irradiance variation, the instantaneous reflection of variation in '*ppv*' on '*ig*' is also associated in the developed controller. The controller also incorporates knowledge of current through the DC link capacitor (icap), whose magnitude is equal to the difference in DC link current and and the current flowing through the winding of motor drive at a time, i.e. *icap= ipv-iph1*. Therefore, the PV reflection component is defined as, the first term in (16), contains the ratio of '*ppv*' to '*Vp*' physically, which represents the maximum amount of supply current against a specific solar output power. The change in the magnitude of '*ppv*' acts as the reflection of variation in insolation level and helps to improve the dynamic performance of the system. Whereas, the term '*VP*' enhances the dynamic response under sudden dip or voltage sag or swell in grid supply. In addition, the term '*icap*' helps to minimize the current through the capacitors. It recognizes the amount of power dissipation in split capacitors and offers small ripples in '*vdc*' under any variation in working conditions by regulating the reference grid current.

IV.   RESULTS & DISCUSSION

The applicability of the proposed system in a real-time environment and to verify the performance, a design of the proposed system is developed in the MATLAB which is illustrated in Fig. 5. The PV simulator is utilized to realize a solar panel of 875 W peak power output to drive a 750W SRM-pump. The designed control logic for grid-side VSC is implemented using a MATLAB implemented controller. The proposed system constitutes three Hall-Effect voltage sensors to sense the DC link voltage, PV output voltage and the voltage across one of the split capacitors, respectively. There are two current sensors, one for PV current and another for grid current sensing are also utilized in the system. A single-phase VSC is used to perform the grid interaction with the system. Other parameters of the proposed system utilized for implementation.
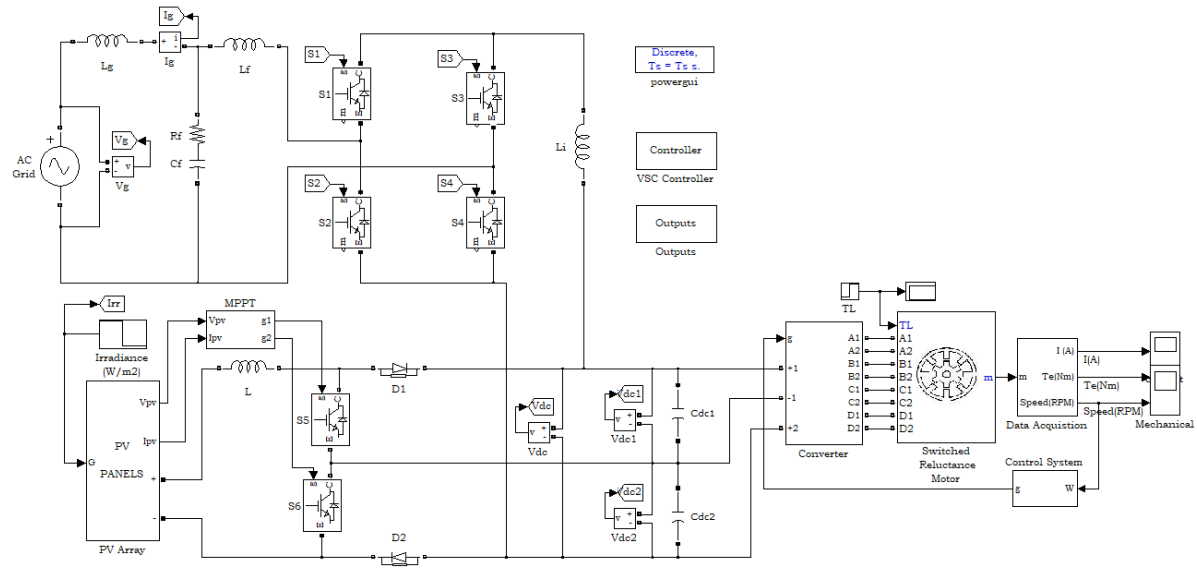
Fig. 5. Simulation diagram of the proposed system

a.   Performance When Only Solar PV Array Runs Pump   Assuming   Grid   is absent or Idle Condition

It is the case   when solar power is adequate to drive the motor at its rated capacity. In this case, the grid is in   floating mode and only helps to keep the DC link voltage at the desired value. The   motor is successfully   soft-started   and   achieved a rated speed   smoothly   as demonstrated in Fig 6 .Similar and   balanced   characteristics of voltages, (vdc1 and vdc2) across   both the split   capacitors are manifested by Fig. 7. Fig. 7 also represents the behavior of current through one of the phases, 'iph1' of SRM. The   nature and magnitude of   stresses   across   all the   indices of TLBC are shown in Fig. The continuous   nature of the inductor current, 'iL' has manifested the CCM operation of   the   MPPT converter. Whereas, the MPPT performance and behavior of 'ppv-vpv' and 'ipv-vpv' curves under this working condition are represented.
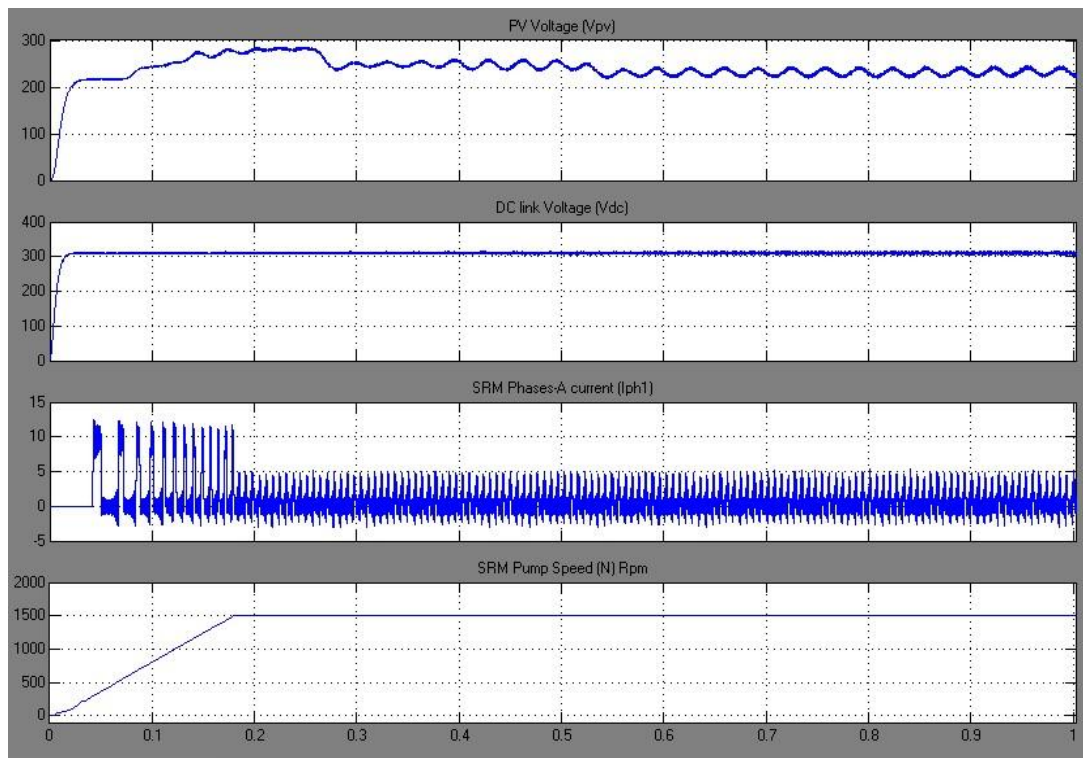

Fig 6 System only when PV array a, Vpv, Vdc, Iph1 and N

b.   Performance When SRM-Pump is run by Grid Only

The situation   when the   water   pumping is   required   in the   night (or the   situation when PV   array   power is not   available),   the   utility grid   is supplying the   required   power   to   the system   for pumping the   full   volume of water. The   characteristics   of grid   and   motor parameters   under   this condition   are   shown in Fig. 8. The grid   current, ig=5.67 A   is   drawn   against the   grid   voltage   of   magnitude   160V   to   fulfill the   power   demand   by   the   load   as demonstrated in Fig. 8. The   drive   is   operating at its   full rated   value   and the pump   is   delivering a full   capacity   of   water as governed Fig. 8. The   characteristics   are   found   satisfactory   by   observing the   indices in   terms of   grid voltage (vg),   grid current (ig),   motor phase current (iph1)   and motor speed (N)   on a   20 ms x-axis   scale.   It   is   shown   in   Fig. 9 (a)   that   the   current drawn   from the   grid is at unity   power factor,   and   has   the   distortion of 4.5%.   Whereas,   the   performance of grid indices   and   harmonic   spectrum of 'ig' are demonstrated in Fig. 9.   All the indices are performing   well and   meet the   IEEE-519 standard.
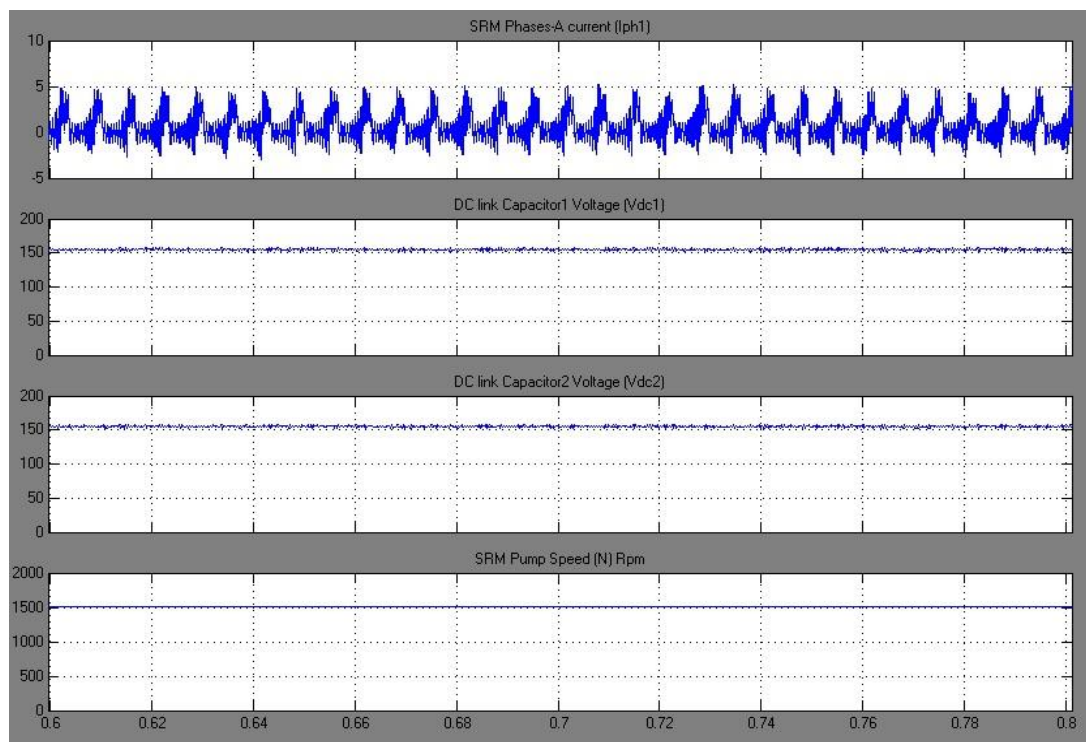

Fig. 7 System only when PV array, Iph1, Vdc1, Vdc2, and N
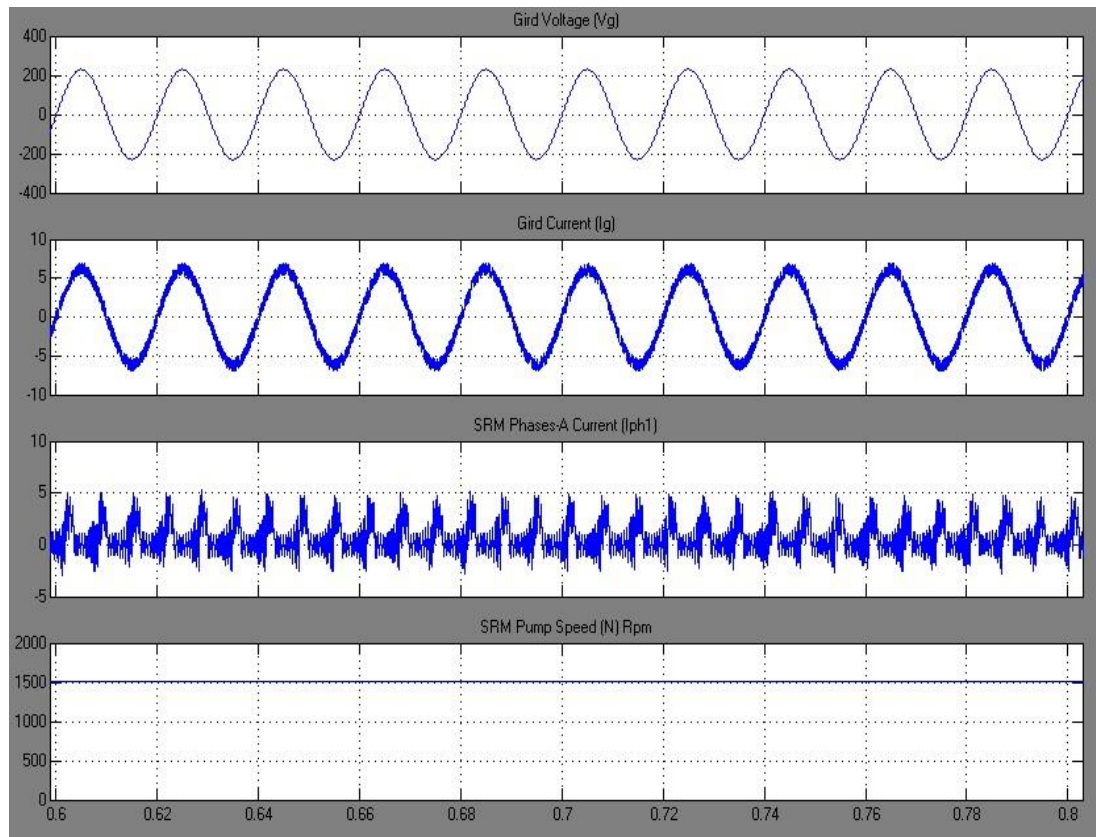
Fig. 8 Performance SRM pump is powered by grid only
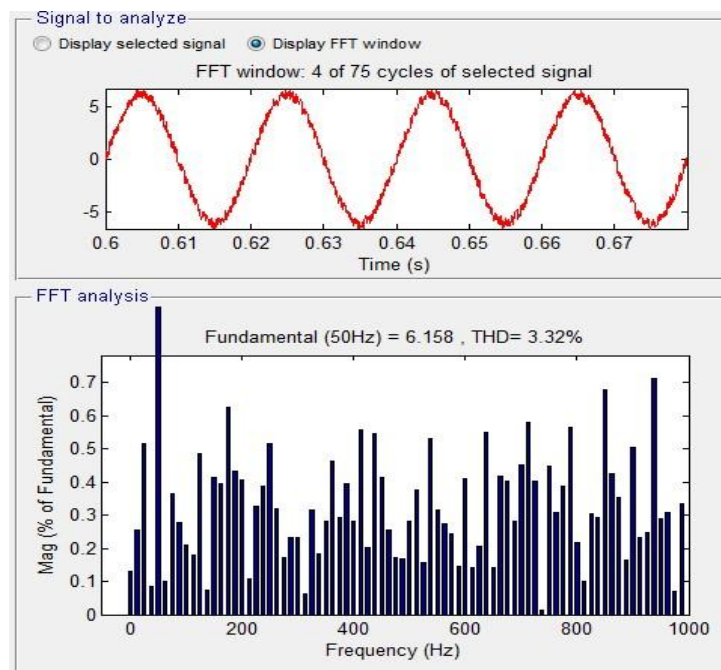

Fig. 9 Performance THD

c.   PV array Power Fed to Grid – Pumping is not required

The control   logic   for   the developed system has   a   provision of feeding the PV power to   the   grid   when   water   pumping is   not   needed.   The behavior of system parameters under this working situation, is illustrated. For a time while, it is considered that a   1000 W/m2 insolation   level is   received   by   the   installed solar panel. The   performance   of PV   array   parameters   and maximum   power   point operation   at   this   insolation   level,   are depicted   in Fig. 10.
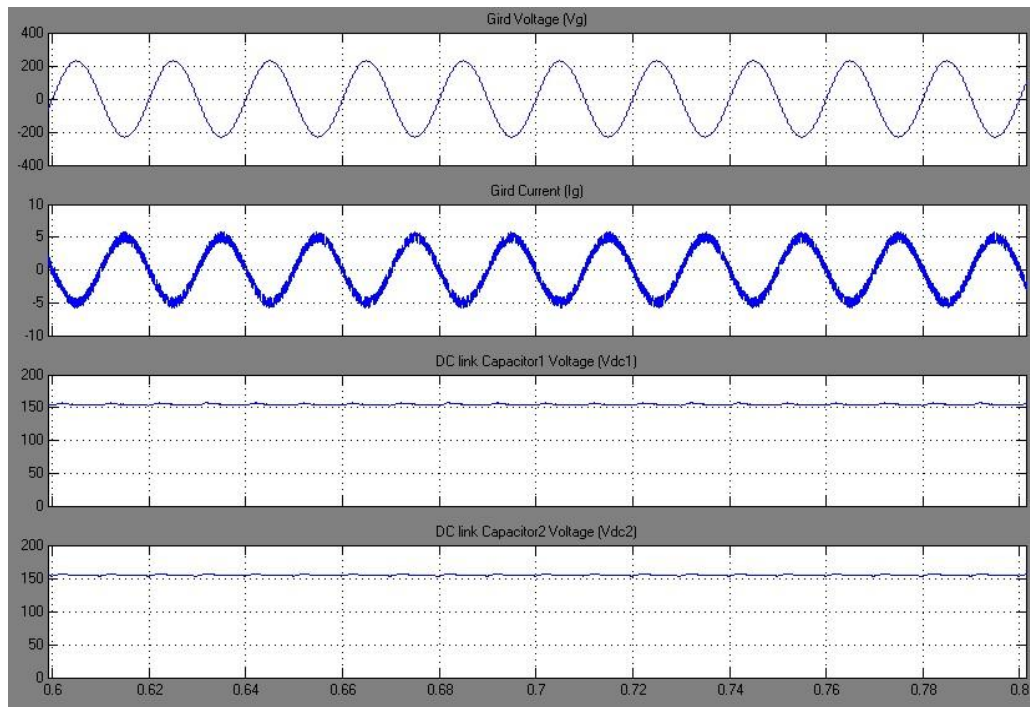
Fig. 10 Steady-state PV array feeds the power to the utility grid

The opposite phase operation of both grid voltage and current demonstrate that the total power generated by the solar panel is fed to the utility grid. It can also be observed that the magnitudes of both the capacitor's voltages 'vdc1' and 'vdc2' are equal. The efficacy of developed control logic for grid-tied VSC and its capability to maintain the power quality according to the IEEE-519 standard is illustrated in Fig. 11.
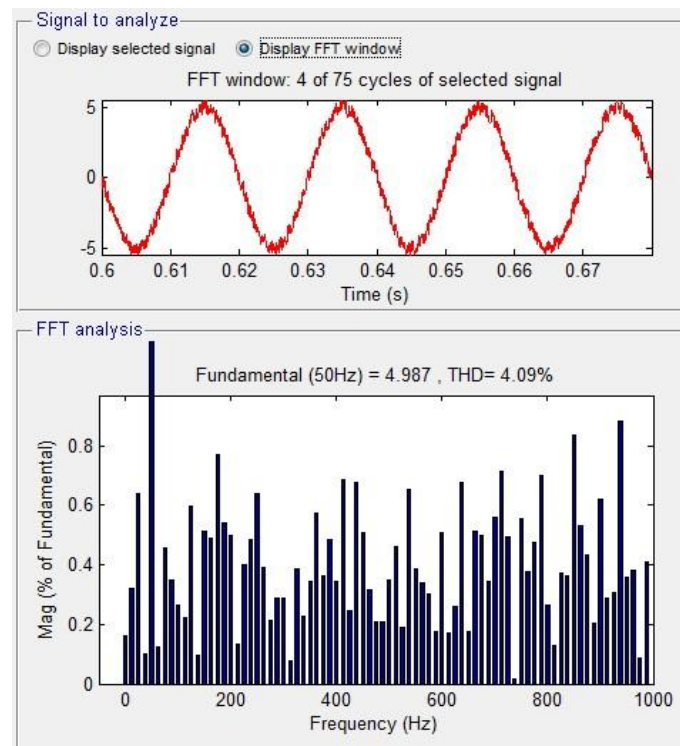

Fig 11. Steady-state PV array THD

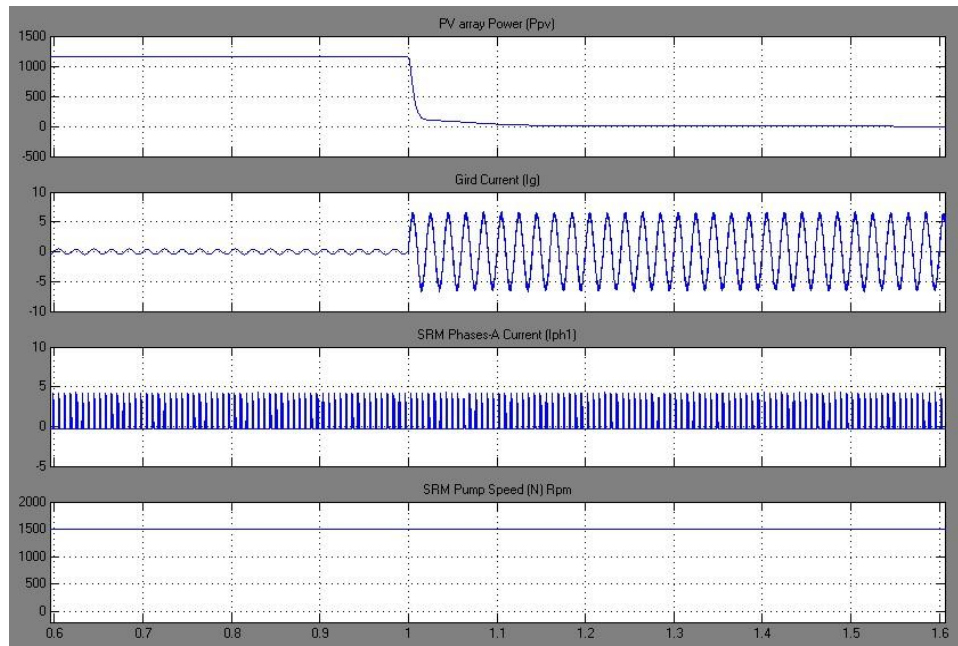**d.   Changeover from PV Array Feeding Pump to Grid Feeding Pump**

Fig 12 Change over from PV array feeding pump to grid feeding pump1

The performance of the system under one of the working situations when PV array power is at its peak value and suddenly goes to zero. In this case, the grid, which has been previously in floating condition supplying the whole power to run the pump. The characteristics   of   different indices are   shown in Fig. 12. It is observed that there is some   momentarily dip in   drive   speed and the grid fulfills   the required power and water pump at full capacity.
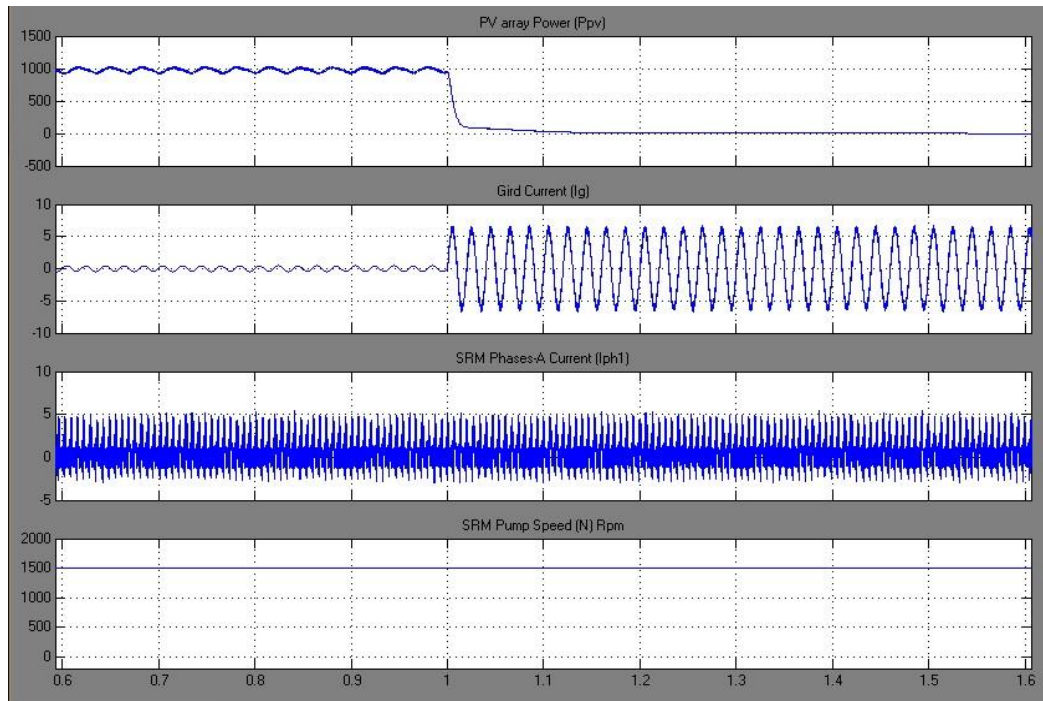

Fig. 13 Changeover from PV array feeding Pump to Grid Feeding Pump

V.   CONCLUSION

A new configuration of a solar-powered water pumping system with the grid support to provide the uninterruptable water supply has been proposed and investigated in this work. It is demonstrated that the developed control for grid-side VSC has performed well under all modes of operation. The proposed control

scheme with the HSTOGI filter is observed to have better stability and good dynamic behavior under sudden variation in working conditions. It has been noted that under all working situations, the DC link voltage is maintained at the desired value except when the grid is not present. In the case when the grid is absent, the system is working simply in standalone mode and the system variable DC link voltage. During the condition when solar power is not sufficient to pump the water at full capacity, the required power is provided by the grid to drive the system at installed capacity. The operation of SRM drive at a fundamental frequency, has been successfully achieved under most of the working time of the developed system and it has significantly contributed to enhancing the performance of the proposed system and minimizes the semiconductor losses. The control implemented through boost converter has been successfully balanced the voltages across the capacitors and maximizes the PV power under all insolation levels.

REFERENCES

[1].   Ministry of New and Renewable Energy, Government of India, 2015-16. *Available: http://www.mnre.gov.in.*
[2].   S. Shukla and B. Singh, "Reduced Current Sensor Based Solar PV Fed Motion Sensorless Induction Motor Drive for Water Pumping," *IEEE Trans. on Industrial Informatics*, vol. 15, no. 7, pp. 3973-3986, July 2019.
[3].   J. V. M. Caracas, G. d. C. Farias, L. F. M. Teixeira, and L. A. d. S. Ribeiro, "Implementation of a High-Efficiency, High-Lifetime, and Low-Cost Converter for an Autonomous Photovoltaic Water Pumping System," *IEEE Trans. Ind. App.*, vol. 50, pp. 631-641, Jan.-Feb. 2014.
[4].   T. D. Short and M. A. Mueller, "Solar-powered water pumps problems, pitfalls, and potential," in *Proc. Inter. Conference on Power Electronics, Machines and Drives, Conf. Publ. No. 487*, 2002, pp. 280-285.
[5].   W. Li, K. Thirugnanam, W. Tushar, C. Yuen, K. T. Chew, and S. Tai, "Improving the Operation of Solar Water Heating Systems in Green Buildings via Optimized Control Strategies," *IEEE Transactions on Industrial Informatics*, vol. 14, no. 4, pp. 1646-1655, April 2018.
[6].   S. Jain, A. K. Thopukara, R. Karampuri, and V. T. Somasekhar, "A Single-Stage Photovoltaic System for a Dual-Inverter-Fed Open-End Winding Induction Motor Drive for Pumping Applications," *IEEE Trans. on Power Electronics*, vol. 30, no. 9, pp. 4809-4818, Sept. 2015.
[7].   M. Huang, "Photovoltaic Water Pumping and Residual Electricity Grid-Connected System," Chinese Patent CN 204131142 U, Jan. 28, 2015.
[8].   C. Slabbert and M. Malengret, "Grid-connected/solar water pump for rural areas," in *Proc. IEEE Inter. Symposium on Industrial Electronics. Proc. ISIE'98 (Cat. No.98TH8357)*, Pretoria, South Africa, 1998, pp. 31-34.
[9].   B. Singh and A. K. Mishra, "Performance analysis of a solar-powered water pumping using improved SIDO buck-boost converter," *IET Power Electronics*, vol. 12, no. 11, pp. 2904-2911, 2019.
[10].   V. Indira Gandhi, R. Selvamathi, and T. Arun Kumar, "Speed control of a switched reluctance motor using PID controller for PV based water pumping applications," in *Proc. Innovations in Power and Advanced Computing Technologies (i-PACT)*, Vellore, 2017, pp. 1-4.
[11].   R. Krishnan, *Switched Reluctance Motor Drives: modeling, simulation, analysis, design and applications*, CRC Press, 2001.
[12].   Y. Hu, C. Gan, W. Cao, C. Li, and S. J. Finney, "Split Converter-Fed SRM Drive for Flexible Charging in EV/HEV Applications," *IEEE Trans. on Industrial Electronics*, vol. 62, no. 10, pp. 6085-6095, Oct. 2015.
[13].   H. Chen, H. Yang, Y. Chen and H. H. Iu, "Reliability Assessment of the Switched Reluctance Motor Drive Under Single Switch Chopping Strategy," *IEEE Transactions on Power Electronics*, vol. 31, no. 3, pp. 2395-2408, March 2016.
[14].   X. Wang, C. Gan, Y. Hu, W. Cao and X. Chen, "Renewable energy-fed switched reluctance motor for PV pump applications," in *Proc. IEEE Conference and Expo Transportation Electrification Asia-Pacific (ITEC Asia-Pacific)*, Beijing, 2014, pp. 1-6.
[15].   A. K. Mishra and B. Singh, "Control of SRM drive for a photovoltaic powered water pumping system," *IET Electric Power Applications*, vol. 11, no. 6, pp. 1055-1066, 7 2017.
[16].   H.M.B. Metwally and W.R. Anis, "Performance Analysis of PV Pumping Systems Using Switched Reluctance Motor Drives," in *Proc. Energy Convers. Mgmt.*, vol.38, no.1, pp.1-11, 1997.